Pressure Vessel Stress Response Under Stationary Operating Loads and Pressure Tests — Measurements on the HDR-RPV and Comparison with Calculations

K. Kussmaul, E. Krägeloh, R. Stegmeyer, J. Jansky
Staatliche Materialprüfungsanstalt (MPA), Universität Stuttgart, Pfaffenwaldring 32, D-7000 Stuttgart 80, Germany

1. SUMMARY

As part of the HDR Safety Program, a cold pressure test (p = 150 bar, T = 50 °C) and a warm pressure test (p = 100 bar, T = 306 °C) of the facility were conducted to verify design and strength calculation. Upset conditions during blowdown and thermal shock loading have been examined.

The instrumentation of the reactor pressure vessel (barrel, head region, head bolts, support) and the connection piping with thermocouples and high-temperature strain gauges allowed the measurements to be decomposed into inner pressure and thermal components. Accompanying theoretical analyses of the RPV and pipes for both load cases showed good agreement with the measured data.

The behaviour of the flange seal could not be experimentally monitored. Nevertheless, according to theoretical considerations which agree well with experimental results from other parts of the structure, there should have never been a loss of tightness during the warmup phase, as a result of the thermal loading (ca. 60 °C/hrs by start-up). This was confirmed.

The measured and calculated strains were compared with the allowable ASME and KTA values. These were never exceeded.

Useful information about critical structure details was obtained for the PHASE II-HDR program, during which the RPV will be intentionally weakened to determine both material and load conditions.

1. INTRODUCTION AND OBJECTIVE

The Superheated Steam Reactor at Grosswelzheim (90 bar, 500°C) with a capacity of 25 MWe represents the prototype of a modified Boiling Water Reactor. With its dimensions of 2960mm inside diameter by 105 (+7mm cladding) wall thickness and length of 12700 mm the HDR pressure vessel, Fig. 1, lies below the dimensions of current 1300 MWe PWR plant (176 bar, 350°C) of 5000mm inside diameter by 243 (+7mm cladding) wall thickness and length of 13250 mm; in which all of the main coolant nozzles are at the same level and are set-on to the flange ring which contains the whole of the reinforcement. For the 1300 MWe Boiling Water Reactor Plant (85 bar, 300°C) with set-through nozzles the dimensions are 6640 mm inside diameter by 163 (+7mm cladding) wall thickness and 22478 mm length.

The cylindrical portion of the HDR pressure vessel was constructed from four forged cylindrical strakes. The reactor pressure vessel (RPV) is closed at its upper end with a closure head by means of 40 studs acting through two flanges and at its lower end by a thick-walled base plate. All of the nozzles attached to the RPV structure are set-on in connection with which only for the large nozzles in the lower region has the basic shell been thickened by about 30%. The RPV is connected to the containment structure via a support frame by means of bolts.

On the material side the vessel does not wholly correspond to present day requirements. With an upper shelf toughness of 100J Charpy V it indeed still lies at the bottom of the scatter band but the NDT-temperature at +15°C is about 30 K too high with respect to the present day requirements for the core region.

The aim of the investigations which were carried out within the compass of the HDR Safety Program is to quantify the safety margins with respect to failure which are present within the structure. To this end as is outlined in Fig. 2, the individual loadings must be determined and compared with the load-bearing capacity of the structure which has possibly been impaired by manufacture or operation.

In the first phase of the HDR Program Investigations were predominantly carried out to determine the loadings under operational conditions (hot pressure test) and test conditions (cold pressure test) or under blowdown conditions (1F-fracture on the steam- or water-side) with or without valve closure. Furthermore the maximum loading which arises in the region of a nozzle during a "pressurised thermal shock" was simulated.

The stresses arising from the individual stages of loading were determined both experimentally (experimental stress analysis) and theoretically (by finite element calculation). In order to obtain information concerning the reliability of the analytical methods currently employed in design, the results obtained were constantly compared.

The investigations on the RPV were concentrated on those regions which by virtue of their geometry acted as points of stress concentration.

In the present paper in the first instance the theoretical (FE-calculation) and experimentally determined stress states under pressure test conditions (cold & hot) are presented for the following regions:

- the cylindrical RPV wall
- the nozzle S
- the closure head flange bolted connection.

Additionally for the closure head flange connection the stress state during hydraulic pre-tensioning is also addressed.

As representative of loading of the RPV structure under upset conditions the stress state at nozzle A1 during blowdown is designated and discussed. Finally the thermal shock-type loading of nozzle A2 is dealt with and assessed.

The theoretical analysis was carried out by means of linear-elastic calculations using the FE program packages ASKA or SMART. The experimental stress analysis was effected using high temperature resistance strain gauges matched to either ferrite or austenite as appropriate.

In view of the unknown residual stresses (following manufacture and previous operation), for all of the stresses which are subsequently discussed it is only a matter of difference values between the loaded and unloaded condition. Moreover it should be noted that whilst mechanical and thermal stresses are admittedly calculated separately, they occur together.

2. STRESSING DURING PRESSURE TEST AND OPERATION; RESULTS FROM MEASUREMENT AND CALCULATION

2.1 Cylinder wall and undisturbed closure head wall-hot

The stressing of the entire vessel was determined theoretically using a two-dimensional, rotationally-symmetrical global analysis without consideration of geometrical discontinuities (e.g. nozzles) in the RPV wall. /1/

As a consequence of its larger thermal expansion on thermal loading, the clad interior of the RPC is compressed. Onto this compression the strain due to internal pressure is superimposed. At the transition to the base and closure head additional constraints (shape compatibility) occur. The maximum thermal stresses in the cladding on the inner wall of the RPV were found to be σ_{Wu} = -400 N/mm^2 approximately; at the RPV outer wall corresponding to the same area only small thermal stresses occured. On superposition of the internal pressure and thermal stresses the global analysis yielded values up to a maximum of σ_u = 200 N/mm^2 (outside) at the points of discontinuity which are considered here.

In one compares the theoretically determined values with the strains measured during the hot pressure test (100 bar, 300°C) /2/ then for the RPV exterior a good agreement may be ascertained, Fig. 3 and 4. On the other hand the strains measured with high temperature strain gauges, matched to

ferrite and located on the RPV interior wall are only in partial agreement with the calculated values, Fig. 4.

2.2 Nozzles - cold and hot

As an example of the stressing of nozzles (hot) nozzle S with an internal diameter of 439mm and wall thickness of 110mm was investigated in detail. The calculations were conducted in the form of a three-dimensional stress analysis /4/.

Here also measurement and calculation are in good agreement on the nozzle exterior, Fig. 5. To be sure the stresses at the nozzle inner edge calculated from the measured strains reproduce the pressure component correctly, however as regards the temperature strains, with ferrite-matched strain gauges higher values should have been measured. As things stand one must assume that a matching error occurd. Strain measurements are to be repeated on the nozzle in 1983.

The maximum circumferential stresses occur at the 0° section (vessel longitudinal direction) with $\sigma_{-u(\Delta T+p_i)}$ = 340 N/mm^2 at the transition between the cladding material and the ferritic (cladding thickness of 7mm assumed).

The measured maximum strains at various nozzles during the cold pressure test, Fig. 6 show that stress concentrations up to α = 3.5 occur within the RPV. The stresses resulting therefrom remain below the limit for secondary stresses (Q form ASME, KTA).

2.3 Closure head flange and studs - cold and hot

The closure head - flange connection together with the seal represents a further problem area which was investigated /6/. As boundary conditions for the calculation of the temperature distribution which should represent the operating conditions in the flanged connection during the "hot" pressure test, the temperatures measured in this region have been used, Fig. 7. For the RPV interior a constant value of 307°C has been estimated although it is known that circulatory currents with variable temperatures were present within the vessel. The temperature distribution within the bolted connection was only calculated using a heat flux over the contact areas between flange and studs, Fig. 8. Radiation was not taken into account.

The flange deformation during the individual phases of loading also resulted from the theoretical investigation. By way of example Fig. 9 shows the deformational behaviour of the flanged connection during cold hydraulic pre-tensioning to 2.7 KN. Here the closure head dome is twisted (flexed) in the contact area opposite to the vessel flange. The closure studs conform to this flexure by bending. The behaviour of the studs is shown in Fig. 10.

For loading cases involving internal pressure and temperature similar deformations were determined. The theoretical results were checked by the mea-

sured strains in the studs and in the flange region and confirmed. The measurements at any given time were taken from studs which were at 90° intervals on the RPV circumference.

The high-temperature strain gauges were applied over half of the stud length. For the loading cases involving hydraulic pre-tensioning, internal pressure and temperature the theoretical and experimental results agreed less well, Fig. 11. This may be attributed to an inadequate comprehension of the temperature distribution.

A comparison of the calculated and measured strains in the region of the closure head flange also shows the same features, Fig. 12 and 13.

2.4 Flange sealing, cold and hot

The leak tightness of the flanged connection, Fig. 14, is determined by the deformation and residual sealing force of the concentric metal O-ring seals. Fig. 15 shows an exaggerated representation of the calculated deformations of the flange surfaces in the sealing region. Under internal pressure loading a maximum opening of 0.087mm occurs at the inner edge of the sealing faces. The lifting-off of the sealing faces extends beyond the inner metal O-ring seal. On superimposing the temperature loading the gap becomes smaller again. However this gaping in none of the loading phases investigated leads to a "leakage gap" since by its elastic resilience and as a result of the impingement of the internal pressure, the O-ring seal can easily bridge the gap which appears and still a residual sealing force remains.

Checking and confirmation of the theoretical results presented here could be achieved by measurements of the strains in the studs and the flange region. These and continuing calculations will serve as a basis for the intended blowdown test in Phase II of the HDR Safety Program.

3. STRESSING DURING BLOWDOWN AND EMERGENCY COOLING

3.1 Blowdown

Of greater interest was the stressing within a nozzle corner during an artificially induced blowdown event (water-side up till 2-phase-flow). This blowdown took place through nozzle A1. The starting temperature of T = 280°C displays a falling tendency down to about 170°C after the commencement of blowdown at various locations on the nozzle corner and circumference. After the discharge and also the intensive cooling of the nozzle inner surface is ended (~65sec) the colder inner surface of the nozzle is reheated from the warmer remainder of the wall, Fig. 16. In accord with the measured temperature histories are the suppressed thermal strains which arise and were also measured, reaching ε_v = 2.1°/oo on the attainment of the maximum temperature difference, Fig. 17. These strains correspond approximately to the

complete suppression of the thermal expansion of the austenitic cladding for $\Delta T = 110$ K ($\alpha = 17.10^{-6} \cdot K^{-1}$)

3.2 Thermal Shock Stressing and Operational Conditions

The thermal shock tests thus far carried our for the simulation of stressing arising from changes of temperature have been of a cyclic nature with a cool down of about $\Delta T = 260$ K and a period of t = 45 sec. The circumferential stresses calculated elastically by means of a 2D-model from the measured temperature history at the nozzle inner wall are given for a wall thickness cross-section in Fig. 18. Comparison of the measured and calculated reference strains (Distortion-energy hypothesis) shows good agreement, Fig. 19.

4. Evaluation of the load cases

The maximum reference strains which arise in the individual load cases investigated are shown in Fig. 20.

The highest strain where $\varepsilon_v = 6$ °/oo was determined during thermal shock loading followed by blowdown with $\varepsilon_v = 2.1$ °/oo. From this it may be deduced that the cold pressure test indeed covers the stresses arising during operation and blowdown but the consequences of thermal shock only if no danger of brittle fracture exists.

5. Evaluation of the design

If one compares the stresses and strains determined by calculation and measurement for the RPV structure with the permissible limit values in accordance with KTA or ASME for

- primary stresses (general membrane stresses, local membrane stresses and bending stresses)
- secondary stresses and
- peak stresses

then it may be seen that all the determined values lie within these limits /7/.

6. Outlook

The preceding investigations have shown that an adequate array of techniques with respect to both testing and strength calculations is available and has been employed appropriately. Consequently the part of the stressing resulting from the loadings (left column in Fig. 2) is thus known so that one is able to delineate the margins of safety for the failure tests (predetermined weakening of the vessel) which are planned for the second phase of the investigation.

The fracture mechanics behaviour is of especial interest since the present RPV-material lies at the lower limit of the currently permissible material toughness. Thus it will be shown to what extent the comparability with other similar materials, such as e.g. KS 01 from the Component Safety Research Program, is confirmed /8/. The thermal shocking facility already proven for local weakening during the 1st phase offers the possibility of producing of enlarging (crack shape, crack depth) pre-determined initial cracks. The removal and examination of the cracked areas (nozzles, cylinder wall) can serve to confirm the previously calculated fracture mechanics quantities.

The pressure required for failure of a nozzle having an inner corner crack (nozzle F) has already been determined using the current customary fracture mechanics failure concepts for a K_{Ic} value of 4464 $N/mm^{3/2}$, Fig. 21.

By carrying out subsequent repair welding under correct procedures at the locations of specimen removal, the integrity of the RPV can be restored so that further testing phases are possible.

For the tests which are now resolved upon it is advisable to refine the strain measurements and inspection measures and to concentrate on those locations where one wishes to introduce points of weakness and undertake fracture mechanics evaluations.

References

/1/ Pfeffer, Stegmeyer: Theoretical stress analysis on the reactor pressure vessel during "hot" pressure test. MPA-Test Report 815 405, January 1982

/2/ Bartonicek, Schöckle: Experimental stress analysis on the reactor pressure vessel and circulation loop during the "hot" pressure test. MPA-Test Report 815 304, August 1980

/3/ Sinz: Damage investigation on high-temperature strain gauges, thermocouples and connected MgO leads. MPA-Test Report 815 305a, February 1978.

/4/ Pfeffer, Stegmeyer: Theoretical stress analysis of Nozzle S of the RPV during the "hot" pressure test, MPA-Test Report 815 405a, January 1982

/5/ Bartonicek, Lang, Schöckle, Zirn: Experimental stress analysis during the "cold" pressure test. MPA-Test Report 815 302, May 1977

/6/ Pfeffer, Stegmeyer: Theoretical stress analysis of the vessel flange-closure head flange with bolting. MPA-Test Report 815 405b, September 1982

/7/ Jansky: Stressing of the HDR pressure vessel under steady operating- and pressure test conditions. Condensed Technical Reports RS 012 J/BS 806

/8/ MPA-Report: TWB1-Material and Weldes Joints. Vol. 1 melts 01 to 07 from August 1981. Author: Sinz et al.

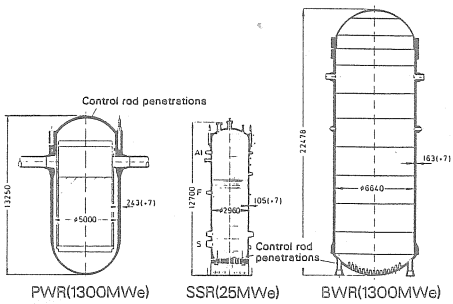

Fig. 1 Comparison of pressurised water-, superheated steam and boiling water reactors.

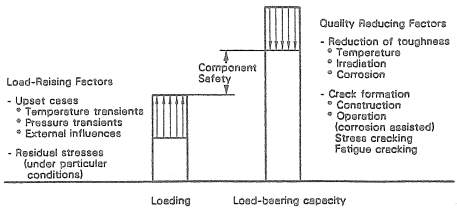

Fig. 2 Definition of safety margin.

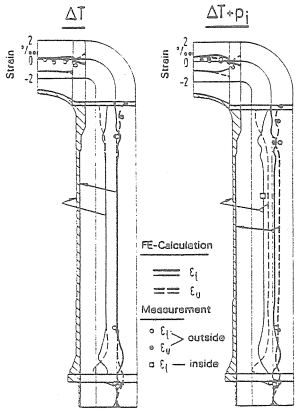

Fig. 3 Calculated longitudinal and circumferential strains along the outer and inner surfaces (cladding) of the pressure vessel in comparison with the measured values.

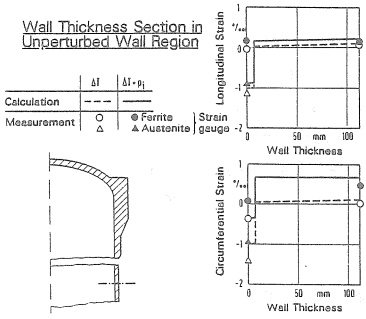

Fig. 4 Variation of the calculated circumferential strain over the wall thickness section B-B (unperturbed wall) compared with the measured strains at the inner and outer surfaces.

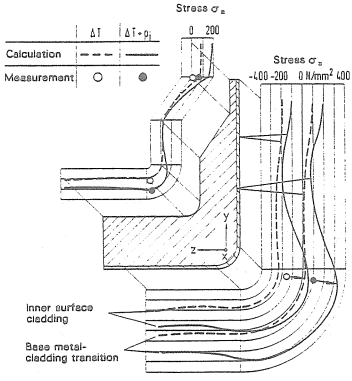

Fig. 5 Variation of the stress σ_x at the outer and inner surfaces and at the ferritic base metal to cladding transition in the 0° nozzle longitudinal section (vessel longitudinal axis direction) of nozzle S.

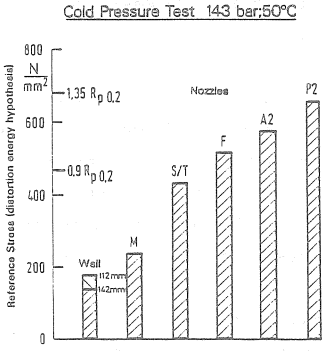

Fig. 6 Maximum reference stresses in the RPV at an internal pressure of 143 bar.

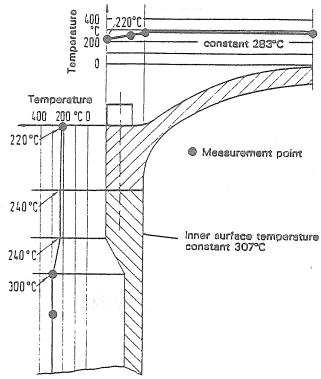

Fig. 9 Considerably exaggerated representation of the deformed flanged connection during hydraulic pre-tensioning.

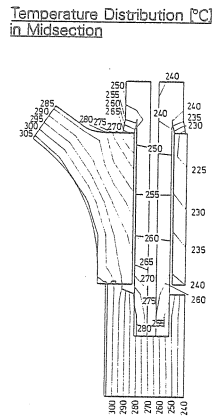

Fig. 10 Variation of longitudinal strain on the inner and outer generatrix of the stud shank after the completed tensioning procedure compared with measurements.

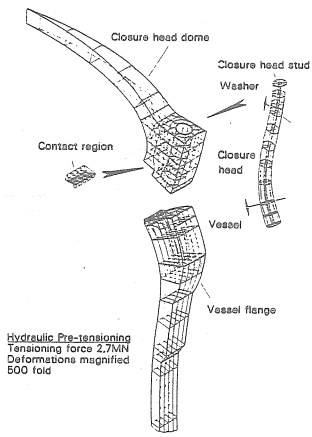

Fig. 7 Temperature profile determined by measurement as boundary condition for the FE temperature field calculation in the region of the closure head flanged connection.

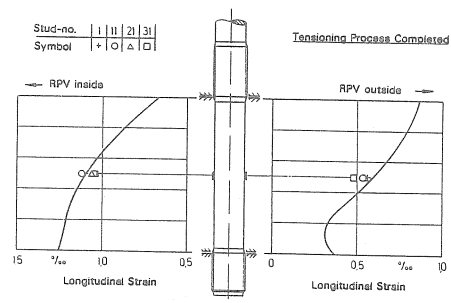

Fig. 8 Isotherms (in °C) in the centre cross-section through the stud (including nut and washer), vessel- and closure head flange.

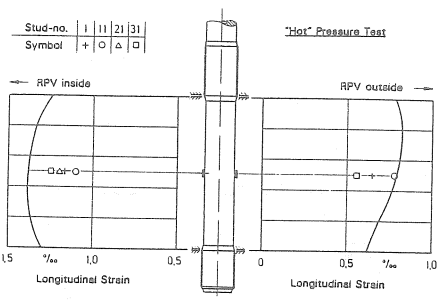

Fig. 11 Variation of longitudinal strain on the inner and outer generatrix of the stud shank under temperature loading, internal pressure and pre-tensioning (hot pressure test) compared with measurements.

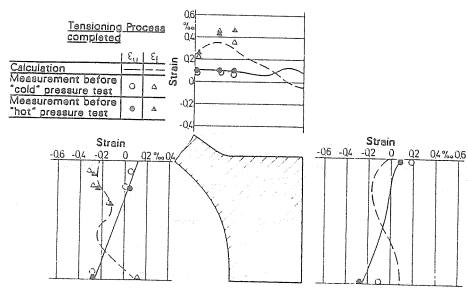

Fig. 12 Variation of the circumferential and longitudinal strain on the inner and outer surfaces of the closure head flange across a radial section after the completed tensioning procedure compared with measurements.

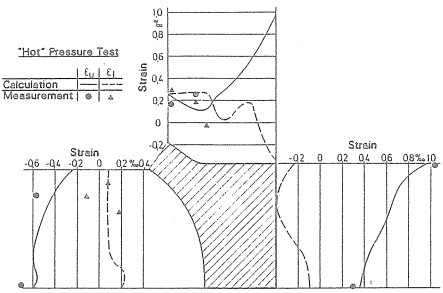

Fig. 13 Variation of the circumferential and longitudinal strain on the inner and outer surfaces of the closure head flange across a radial section under temperature loading, internal pressure and pre-tensioning (hot pressure test) compared with measurements.

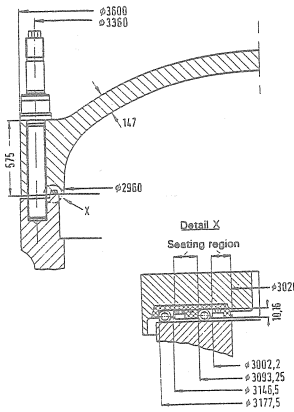

Fig. 14 Main dimensions of the flanged connection including the sealing region.

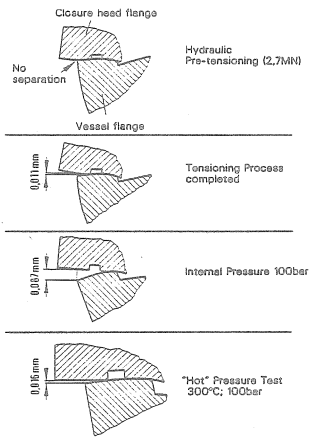

Fig. 15 Exaggerated representation of the deformations in the sealing region for the loading phases investigated.

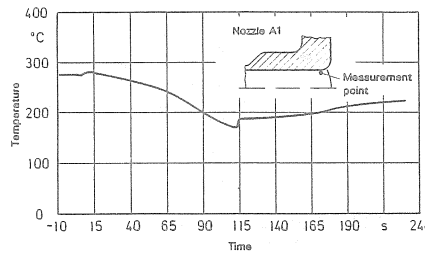

Fig. 16 Temperature variation at the inner wall of the RPV discharge nozzle (blowdown nozzle A1) - measured at the nozzle corner.

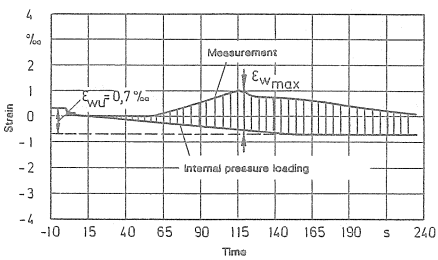

Fig. 17 Divergence of the measured circumferential strains at the inner corner of the discharge nozzle A1 under internal pressure and thermal loading.

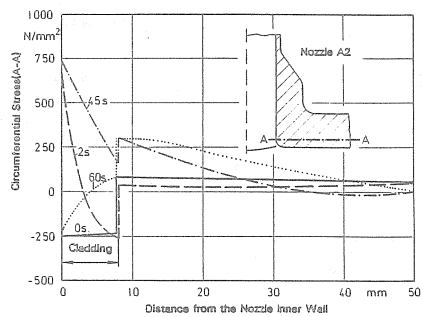

Fig. 18 Linear- elastically calculated circumferential stresses across a wall thickness section of the A2 nozzle under thermal shock loading (T = 260 K, cooling time = 45 sec).

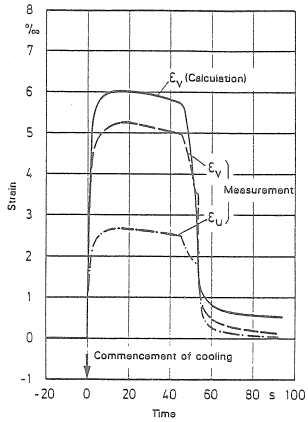

Fig. 19 Comparison of the calculated reference strain with that determined from measurements at the inner corner of the A2 nozzle under thermal shock loading (t = 45 sec).

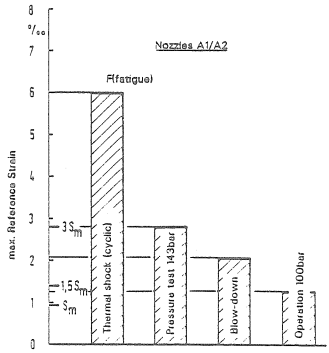

Fig. 20 Quantification of the individual loading cases. (F-peak stress in accordance with ASME-BPVC Section III)

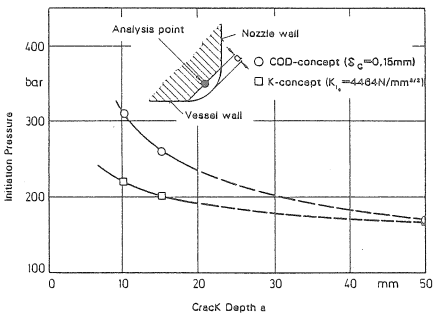

Fig. 21 Initiation pressures for nozzle F determined in accordance with fracture mechanics failure concepts.